CHALMERS

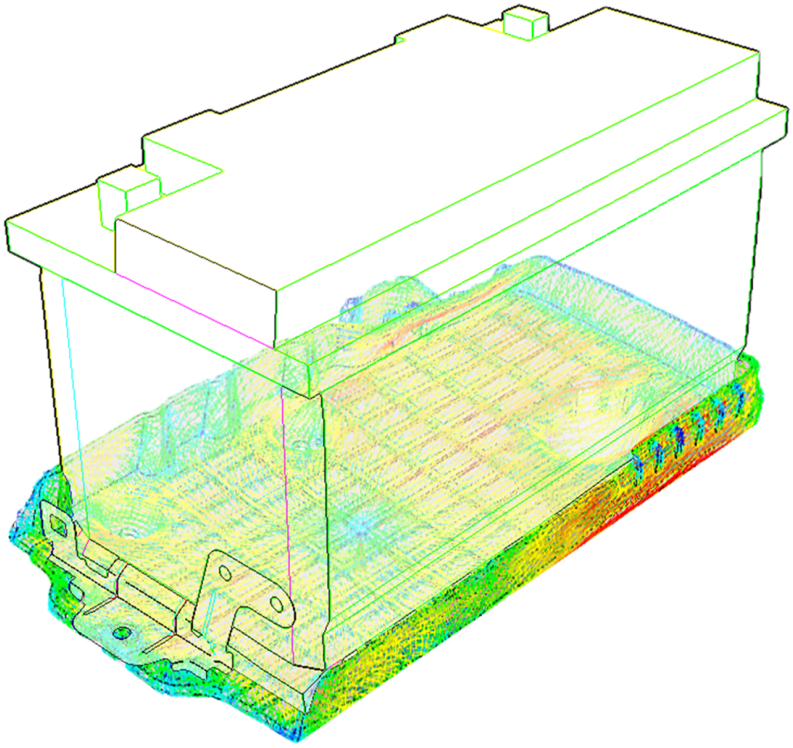

Coupling of Injection Moulding Process to Stress Analysis of Short Fibre Composite Structures

Master's thesis in Applied Mechanics

VCC Report No. Dura-CAE-2012-080

JENNY CARLSSON

Department of Applied Mechanics
Division of Material and Computational Mechanics
CHALMERS UNIVERSITY OF TECHNOLOGY
Gothenburg, Sweden 2012
Master's thesis 2012:12

MASTER'S THESIS IN APPLIED MECHANICS

Coupling of Injection Moulding Process to Stress Analysis of Short Fibre Composite Structures

JENNY CARLSSON

Department of Applied Mechanics

Division of Material and Computational Mechanics

CHALMERS UNIVERSITY OF TECHNOLOGY

Gothenburg, Sweden 2012

Coupling of Injection Moulding Process to Stress Analysis of Short Fibre Composite Structures
JENNY CARLSSON

Master's thesis 2012:12
ISSN 1652-8557
Department of Applied Mechanics
Division of Material and Computational Mechanics
Chalmers University of Technology
SE-412 96 Gothenburg
Sweden
Telephone: +46 (0)31-772 1000

Cover:
Fibre orientation plot of the battery tray with the rest of the set up outlined

98450 TDS Print Volvo Car Corporation
Gothenburg, Sweden 2012

Coupling of Injection Moulding Process to Stress Analysis of Short Fibre Composite Structures
Master's thesis in Applied Mechanics
JENNY CARLSSON
Department of Applied Mechanics
Division of Material and Computational Mechanics
Chalmers University of Technology

Abstract

Adding short glass fibres to polymers is a common way to increase the stiffness and strength of injection moulded components. This thesis is concerned with structural analysis of injection moulded short fibre composites, using injection moulding simulations to establish the fibre orientation state. In the traditionally employed approach short fibre composites are assumed to be more or less isotropic. As is shown in this thesis this is not always the case, and tensile testing of injection moulded test pieces leads to an overestimation of both stiffness and strenght of such components.

For linear elastic stiffness analysis there are well working interfaces between the injection moulding and structural analysis softwares. For strength analysis a Matlab programme has been written, which uses a method suggested by Laspalas et al. [1] to establish the fibre dependent strength properties, together with the Hill criteria for predicting failure.

For a test piece according to ISO 527 [2], the correlation between simulation and test data is good with regards to both stiffness and strength. The injection moulding simulation results show a high level of fibre orientation in the length direction of the test piece, indicating that stiffness and strength properties established from tensile tests of such test pieces are overestimated.

Analysis of more complex geometries show that the Youngs modulus established in tensile tests or tensile test simulations of test pieces is highly overestimated. In an analysis of a battery tray mounted with a battery, the deflection measured when using a material model which consideres the fibre orientation was a factor 1.8 larger than when assuming that the material is isotropic and using the Youngs modulus obtained in tensile testing of an ISO 527 test piece.

Keywords: Anisotropy, Composite processing, Elastic properties, Fibre orientation, Injection molding, Short fibre composites, Strength, Stress

Preface

This Master thesis was written during the spring of 2012 as the final part of the Master's Programme in Applied Mechanics at Chalmers University of Technology. The work has been carried out in the department for CAE Durability at Volvo Car Corporation. Ph.D. Magnus Oldenbo of Volvo Car Corporation has supervised and Ragnar Larsson, Professor in Computational Material Mechanics at Chalmers, has been the examiner.

Acknowledgements

I would like to thank all my colleagues at Volvo Car Corporation, CAE Durability, and especially my supervisor Magnus Oldenbo for help and support. In addition I would like to express my gratitude to Mohsen Hessami at NTI CADcenter for all the help with Moldflow and for patiently trying to answer my questions about the fibre orientation solver, and to Lars Wikander at Volvo IT for setting up the computer environment. Finally, I would like to thank my family and friends for support, input and proofreading.

Gothenburg May 2012
Jenny Carlsson

Nomenclature

E_i	Youngs modulus in direction i
E_f	Youngs modulus of fibre
E_m	Youngs modulus of matrix
V_f	Volume fraction fibre
V_m	Volume fraction matrix
ν_{ij}	Poissons ratio relating strain in direction i to strain in direction j
ν_f	Poissons ratio of fibre
ν_m	Poissons ratio of matrix
G_{ij}	Shear modulus in direction j on the plane whose normal is in direction i
G_f	Shear modulus of fibre
G_m	Shear modulus of matrix
σ_{ij}	Stress tensor
σ_i	Stress tensor in Voigt form
ϵ_{ij}	Strain tensor
ϵ_i	Strain tensor in Voigt form
C_{ijkl}	Fourth order stiffness matrix
C_{ij}	Stiffness matrix in Voigt form
S_{ij}	Compliance matrix in Voigt form
$S_{ij,\text{plane stress}}$	Compliance matrix for state of plane stress
Q_{ij}	Stiffness matrix for state of plane stress
E_{random}	Youngs modulus for composite with random orientation
A, A_{1-5}	Parameters used in the Tandon-Weng [3] micromechanical model
$\boldsymbol{C}_f$	Stiffness matrix of the fibre material
$\boldsymbol{C}_m$	Stiffness matrix of the matrix material
S_{ijkl}	The Eshelby tensor
$\boldsymbol{E}_m^0$	The modified Eshelby tensor in Eduljee et al. [4] micromechanical model
A_{ij}	The second order fibre orientation tensor, a.k.a. orientation state tensor
A_{ijkl}	The fourth order fibre orientation tensor
a_{11}	First element of A_{ij}. See subsection 2.2.3 for more detail.
f_p	Orientation parameter used in Eduljee et al. [4] micromechanical model
g_p	Orientation parameter used in Eduljee et al. [4] micromechanical model
$\boldsymbol{p}$	Vector describing the orientation of one fibre
ψ	Fiber orientation probability density function
W_{ij}	Vorticity tensor of flow
D_{ij}	Deformation tensor of flow
ξ	Shape parameter in flow
Ci	Coefficient of interaction beween fibres in flow
$\dot{\gamma}$	Shear rate of flow
δ_{ij}	Kronecker delta
κ	Reduced strain coefficient
L_{ijkl}	Function of the orientation state tensor A_{ij}
M_{ijkl}	Function of the orientation state tensor A_{ij}
C_{ij}	Function of the orientation state tensor A_{ij} and D_{ij}. Only in section 2.4.
F_{ij}^{ud}	Strength matrix of unidirectional material
$\bar{\sigma}_{cl}$	Strength in longitudinal direction, averaged over fiber length distribution

σ_{cl}	Strength in longitudinal direction
σ_{ct}	Strength in transverse direction
τ	Shear strength
σ_f	Strength of fibre
σ_m	Strength of matrix
F_{ij}	Strength matrix for the oriented material
σ	Apparent stress in test piece
F	Resultant force in test piece
A	Cross sectional area of test piece
ϵ	Engineering strain of test piece
l_1	Undeformed length of test piece
l_2	Deformed lenght of test piece
E	Apparent Youngs modulus of test piece

Abbreviations

AR	Aspect Ratio
ARD	Anisotropic Rotary Diffusion model
CAE	Computer Aided Engineering
FE	Finite Element
FEM	Finite Element Model
MFD	Melt Flow Direction
MSA	Moldflow Structural Alliance
ORF	Orthotropic Fitted closure model
RSC	Reduced Strain Closure model
SFC	Short Fibre Composite
VCC	Volvo Car Corporation

Contents

Abstract i

Preface iii

Acknowledgements iii

Nomenclature v

Abbreviations vi

Contents vii

1 Introduction 1
1.1 Background . . . 1
1.2 Objective . . . 3
1.3 Delimitations . . . 3
1.4 Method . . . 3

2 Theory 5
2.1 Composite materials . . . 5
2.2 Micromechanical models . . . 6
2.2.1 Random orientation . . . 7
2.2.2 Tandon-Weng model . . . 8
2.2.3 Eduljee, McCullough and Gillispie model . . . 9
2.3 Injection moulding simulation . . . 10
2.4 Fibre orientation . . . 10
2.5 Strength . . . 13
2.5.1 Ultimate strength estimation . . . 14
2.5.2 Failure criterion . . . 14

3 Analyses 15
3.1 Solver, interface and other software . . . 15
3.1.1 Moldflow . . . 15
3.1.2 Abaqus . . . 16
3.1.3 Moldflow Structural Alliance . . . 16
3.1.4 Matlab . . . 16
3.2 Celstran PP-GF50 . . . 17
3.3 Structural FE models and preprocessing . . . 18
3.3.1 Test piece . . . 18
3.3.1.1 Strength analysis . . . 18
3.3.2 Plate with hole . . . 19
3.3.3 Case study: Battery tray . . . 20

4 Results 22
4.1 Linear elastic analysis . . . 22
4.1.1 Test piece . . . 22

4.1.1.1 Process induced stress 24
4.1.2 Square with hole 24
4.2 Strength analysis 25
4.3 Case study: Battery tray 27

5 Discussion **29**
5.1 Stiffness 29
5.2 Strength 29
5.3 Process induced stress 30
5.4 Interface and solvers 30

6 Suggestions for further work **32**

7 Conclusions **33**

8 List of Figures **34**

9 List of Tables **34**

10 References **35**

1 Introduction

In order to make cars lighter without compromising demands on durability, safety and comfort, new materials are constantly developed and existing ones refined. One measure that can be taken is to increase the amount of composites in the car, and only use steel when its specific properties are required. This thesis is concerned with modelling and analysing discontinuous fibre polymer composites, which are the result of injection moulding plastics reinforced with short (∼0.5–12 mm long) glass fibres. These fall into the category short fibre composites (SFC).

One important aspect of weight reduction is fuel consumption. In later years, awareness of the human impact on the greenhouse effect has increased, and so has fuel prices. During the period 2000–2011, Volvo lowered the average fuel consumption of new cars by more than 25 % [5]. By making the cars lighter, fuel consumption is automatically lowered which is a competitive advantage when consumers are environmentally concerned and economical incentives are used to encourage people to buy eco-friendly cars.

1.1 Background

The injection moulding process consists of four steps, see Figure 1.1.1. First the plastic raw material, usually in the form of pellets, is fed into the machine through the hopper. The plastic is then pushed forward by the screw in the extruder. Here the plastic is melted due both to heat and friction. The plastic melt is injected into the comparatively cool mould, the pressure is held for some time until the part is sufficiently frozen and the part is then ejected.

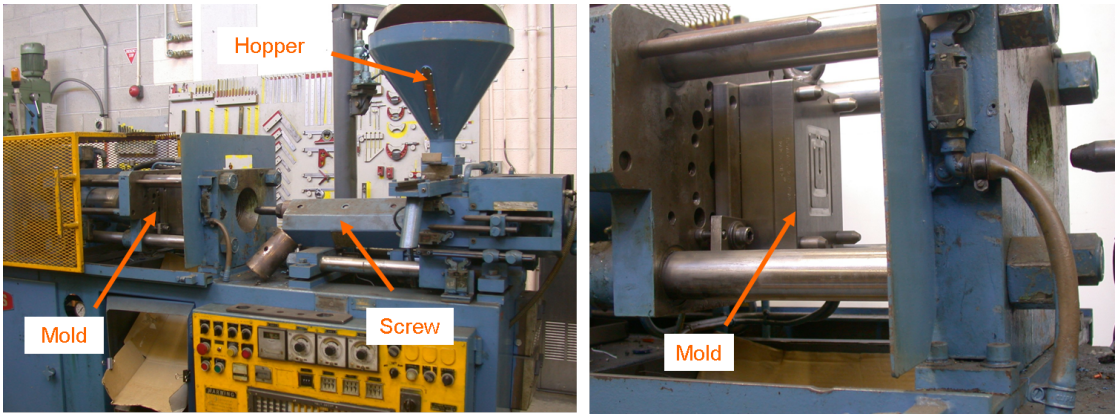

Figure 1.1.1: *Small injection moulding machine used for injection moulding of paper clips.*[1]

In order to increase the stiffness and strength of the moulded product, glass fibres can be added to the mixture. The fibres are included in the pellets. During injection moulding the fibres never melt but follow the flow of molten plastic into the mould. The finished

[1] Photographs taken by Glenn McKechnie, cc-by-sa-2.5 2005.

product is a composite. It consists of two distinct components, the fibres and the plastic surrounding it, called the matrix. Fibres tend to align themselves depending on the flow direction. Near the walls of the mould, where the flow is of a shearing nature, the fibres tend to align themselves along the flow direction whereas closer to the core of the mould, where the shear is significantly less, the fibres are more randomly of even transversely oriented [6].

The traditionally employed approach when performing structural analysis of injection moulded SFC is to assume that the material is isotropic and use the material properties found in data sheets. This apporach presupposes that the fibre orientation is completely random, or that the orientations cancel out over the thickness. An overview of avaliable research shows that this is not the case [1, 7]. Moreover, higher amounts of fibre leads to an increased anisotropy, whereas longer fibres leads to a lower level of anisotropy [8].

In general the mechanical properties of short fibre composites are determined through tensile testing of injection moulded test pieces such as the one in Figure 1.1.2. The procedure for producing and testing such a test piece is described in standards such as [2]. The test piece is produced either as a large sheet with a distributed film gate along one edge from which test pieces of the correct geometry are cut, or by injection moulding the correct geometry with a gate in one end of the test piece. In both cases fibres tend to align themselves more in the length direction of the test piece than in the transverse direction, which can cause the stiffness and strength of the material to be overpredicted.

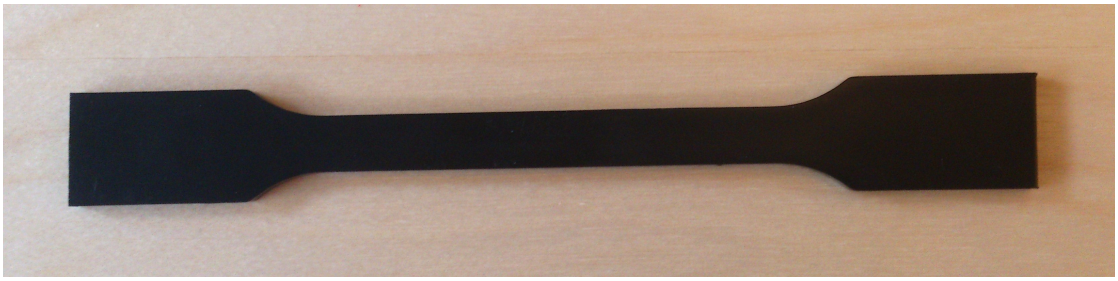

Figure 1.1.2: *Injection moulded test piece used for tensile testing.*

Bernasconi et al. [7] used a large sheet of polyamide-6 injection moulded with a distributed film gate and cut test pieces of identical geometry but with different angles relative to the melt flow direction (MFD). Their results show that the stiffest and strongest direction, which was the direction of the flow, was twice as stiff as the weakest direction, and 1.7 times as strong. Comprehensive material data sheets from a supplier show that Youngs modulus differ a factor 1.5–1.6 between the flow direction and the transverse direction [9]. Overprediction of stiffness is also the background for the work by Grauers [10], who has investigated why a short fibre composite bumper beam did not perform as well in physical testing as in simulations. Her main conclusion was that the stiffness was overpredicted in the material data used for the simulations as compared to the actual bumper beam.

1.2 Objective

The purpose of this thesis is to investigate how injection moulding simulations in Autodesk Moldflow can be used in stiffness analysis of injection moulded short fibre composite components. The method should be applicable on real components. The thesis work will also investigate how to evaluate strength considering the process induced anisotropy of the materials.

1.3 Delimitations

This work is at an early development stage and no ready to use method is expected; the aim is to formulate the framework for such a method. Further development will be needed before this can be used as a standard method at Volvo Car Corporation (VCC).

1.4 Method

The injection moulding simulation tool used will be Autodesk Moldflow Insight Basic, as this is the more advanced injection moulding simulation software used within VCC. The primary finite element (FE) analysis tool is Simulia Abaqus and for the interface between Moldflow and Abaqus, Autodesk Moldflow Structural Alliance (MSA) is used. There are other options such as Simulia's Abaqus Interface for Moldflow or the Dutch programme Digimat but these will not be reviewed, see chapter 6 for reflections on these. Moldflow does not compute ultimate strength of the composites; for this purpose a custom written program using Matlab and the Calfem package is developed in the thesis work and used.

Figure 1.4.1 describes the overall work flow of the stress analyses involving the manufacturing induced material properties. First the FE model is set up in a preprocessor such as Abaqus CAE or Ansa. The geometry is then exported from Abaqus CAE, using MSA, to Moldflow where the injection moulding simulation is performed. In the injection moulding simulation the flow of the plastic melt is predicted. The injection moulding simulation also includes predicting the fibre orientation state. Moldflow computes the material parameters (Youngs modulus, Poissons ratio and shear modulus) of a hypothectical, fully aligned, material using a micromechanical model. These properties are then combined with the fibre orientation data (principal directions and level of orientation) to obtain the resulting orthotropic material properties of each element. The material properties are then used, through MSA, by Abaqus for structural analysis. Alternately mesh and fibre orientation is exported to Matlab, where material properties are calculated and the FE problem is set up and solved. The stresses are then compared to an orthotropic failure criterion to evaluate when failure will occur.

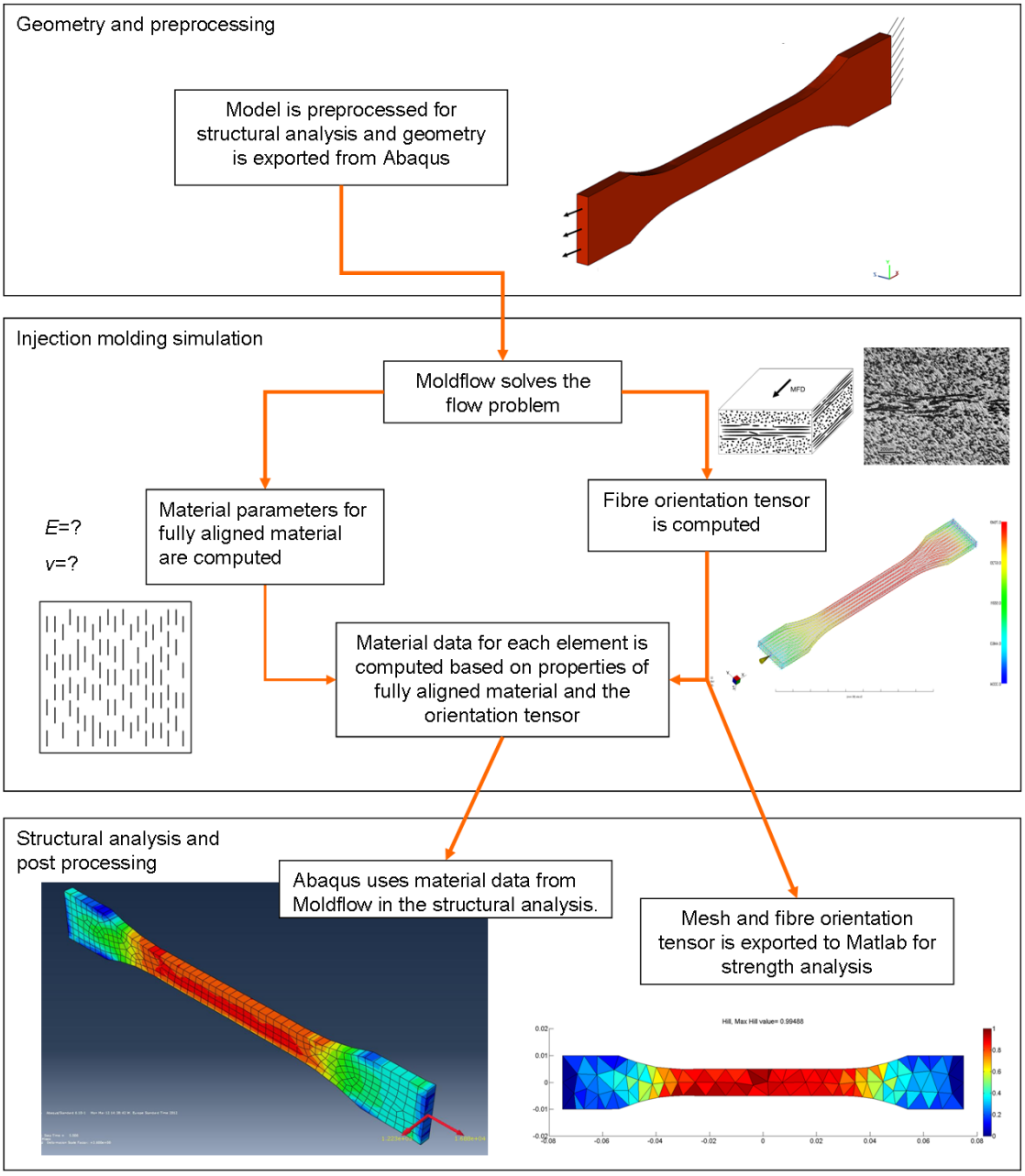

Figure 1.4.1: *Work flow of the analyses: First the model is preprocessed in a preprocessor. The geometry for the injection moulding simulation is then exported to Moldflow where the injection moulding simulation is performed. Here fibre orientation and material properties are computed. These material properties are then used in the structural analysis in Abaqus. Alternately, mesh and fibre orientation are exported to Matlab, where material properties are computed and the finite element problem is set up and solved. The stresses obtained are then used with a failure criterion to predict failure.*

2 Theory

Some of the main theories and methods used in this work are presented, beginning with some general issues on composite materials and how mechanical properties of composites are determined. After that follows a brief description of the theories used within Moldflow for simulating flow and determining fibre orientation as well as resulting mechanical properties. The last part deals with ultimate strenght of composites in general and SFC in particular.

2.1 Composite materials

A composite can be defines as:

> "A macroscopic combination of two or more distinct materials into one with the intent of suppressing undesirable properties of the constituent materials in favour of desirable properties." [11]

By this definition adding short glass fibres to a thermoplastic matrix in order to enhance the mechanical properties of the thermoplastic creates a composite.

There are several kinds of composites, not just the unidirectional laminates based on carbon or glass fibres which are perhaps the most well known. This thesis deals with short fibre composites. In general a fibre composite can be described by two parameters or extremes; (a) if it consists of continuous or discontinuous fibres and (b) if the fibres are unidirectional or randomly oriented, see Figure 2.1.1. Aspect ratio (AR) is a concept used to describe the relative length of fibres. AR of a fibre is computed as $AR = \frac{l}{d}$, the lenght of the fibre over the cross sectional diameter. Spherical inclusions, for example, have AR=1. Continuous fibres have AR approaching infinity. Inclusions can also be lamellar with AR approaching zero. AR of the fibres in the discontinuous composites studied is about 100 [8].

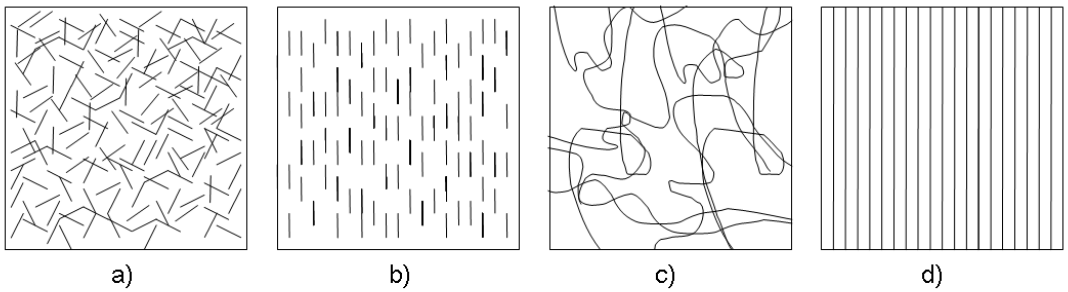

Figure 2.1.1: *Different types of fibre composites: a) Randomly oriented discontinuous fibres, b) Aligned discontinuous fibres, c) Randomly oriented continuous fibres and d) Aligned continuous fibres.*

In the same way composites are rarely entirely unidirectional, nor completely randomly oriented, through the thickness of a component. Fibres can be woven like a fabric or stacked up by laminae, which in themselves are approximately unidirectional, but with different stacking angles. When injection moulding discontinuous fibre composites the fibres tend to orient themselves according to the flow, but the fibres are not completely aligned. Depending on geometry and processing conditions they can be close to random or highly oriented. In this thesis the concept aligned or unidirectional is used for completely aligned composites, whereas oriented refers to the fibre orientation state obtained in the injection moulding process which is neither random, nor aligned, and dependent on the geometry of the mould.

In the following chapters all discontinuous fibre composites will be referred to as SFC even though the manufacturer refers to the material studied as "long glass fibre filled polypropylene". Fibres of a length of approximately 10 mm before processing are called long since they are long compared to most injection moulded composites ($AR = 30$ is a commmon aspect ratio [7, 8]), but for the rest of this thesis "short" refers to all discontinuous fibres.

2.2 Micromechanical models

A micromechanical model is used to predict the mechanical properties of a composite based on the properties of the constituents. One of the simplest micromechanical models is the rule of mixtures, in which the properties of a unidirectional lamina are predicted as

$$E_1 = E_f V_f + E_m V_m \tag{2.2.1}$$

$$\frac{1}{E_2} = \frac{V_f}{E_f} + \frac{V_m}{E_m} \tag{2.2.2}$$

$$\nu_{12} = \nu_f V_f + \nu_m V_m \tag{2.2.3}$$

$$\frac{1}{G_{12}} = \frac{V_f}{G_f} + \frac{V_m}{G_m} \tag{2.2.4}$$

Principal direction 1 is the fibre direction, and indices f and m refer to fibre or matrix property respectively. V_f is the volume fraction of fibre and V_m is the volume fraction of the matrix. Since the composite studied has only two constituents, $V_m + V_f = 1$. For a more thorough derivation of these relations see for example [11].

The anisotropic mechanical properties can be used to set up the stiffness matrix C_{ijkl}, which gives the constitutive relation of the material

$$\sigma_{ij} = C_{ijkl}\epsilon_{kl} \tag{2.2.5}$$

C_{ijkl} is a 3×3×3×3 matrix and has thus 81 components which, through symmetry of both stress and strain, can be reduced to 36 independent components such that equation 2.2.5 can be rewritten, using Voigt notation, as

$$\sigma_i = C_{ij}\epsilon_j \tag{2.2.6}$$

Here C_{ij} is a 6×6 matrix and σ and ϵ are 6×1 vectors. The inverse of the stiffness matrix, S_{ij}, is characterized by the relation

$$\epsilon_i = S_{ij}\sigma_j \tag{2.2.7}$$

and S_{ij} is called the compliance matrix. In case of transversal isotropy, where 1 is the fibre direction, the compliance matrix has the form

$$S_{ij} = \begin{bmatrix} 1/E_1 & -\nu_{21}/E_2 & -\nu_{31}/E_3 & 0 & 0 & 0 \\ -\nu_{12}/E_1 & 1/E_2 & -\nu_{32}/E_3 & 0 & 0 & 0 \\ -\nu_{13}/E_1 & -\nu_{23}/E_2 & 1/E_3 & 0 & 0 & 0 \\ 0 & 0 & 0 & 1/G_{23} & 0 & 0 \\ 0 & 0 & 0 & 0 & 1/G_{31} & 0 \\ 0 & 0 & 0 & 0 & 0 & 1/G_{12} \end{bmatrix} \tag{2.2.8}$$

For the state of plane stress the compliance matrix can be directly reduced, by removing the appropriate rows and columns in Equation 2.2.8, to

$$S_{ij,\text{plane stress}} = \begin{bmatrix} 1/E_1 & -\nu_{21}/E_2 & 0 \\ -\nu_{12}/E_1 & 1/E_2 & 0 \\ 0 & 0 & 1/G_{12} \end{bmatrix} \tag{2.2.9}$$

The inverse of this reduced compliance matrix is the stiffness matrix applicable for the state of plane stress. It is often referred to as the lamina stiffness matrix and has the form

$$Q_{ij} = S^{-1}_{ij,\text{plane stress}} = \frac{1}{1-\nu_{12}\nu_{21}} \begin{bmatrix} E_1 & \nu_{21}E_1 & 0 \\ \nu_{12}E_2 & E_2 & 0 \\ 0 & 0 & G_{12}(1-\nu_{12}\nu_{21}) \end{bmatrix} \tag{2.2.10}$$

Note that this is not the same matrix as would have been obtained by removing rows and columns in the stiffness matrix, which is why it is no longer referred to as C_{ij}. For a more thorough derivation of these relations see for example [12].

2.2.1 Random orientation

Youngs modulus for a composite can be estimated using the rule of mixtures for the aligned material, together with a fibre orientation distribution function. For a completely random distribution of fibres the distribution function is constant, as the distribution is

equal in all directions. By integrating over the angular domaine, one obtains the Youngs modulus for a composite with random orientation as [11]

$$E_{\text{random}} = \frac{1}{\pi}\int_{-\pi/2}^{\pi/2} E_x(\theta)\psi(x,y)d\theta = \{\psi(x,y)=1\}... = \frac{3}{8}E_1 \tag{2.2.11}$$

2.2.2 Tandon-Weng model

The rule of mixtures provides a quick estimate of the properties of unidirectional laminae but for more exact applications, and especially for SFC, it is insufficient. Therefore a more complex micromechanical model is used within Moldflow, namely the model suggested by Tandon and Weng [3]. In the Tandon-Weng micromechanical model the mechanical properties of a material with aligned elipsoidal inclusions are calculated as

$$\frac{E_1}{E_m} = \frac{1}{1+V_f(A_1+2\nu_m A_2)/A} \tag{2.2.12}$$

$$\frac{E_2}{E_m} = \frac{E_3}{E_m} = \frac{1}{1+V_f[-2\nu_m A_3+(1-\nu_m)A_4+(1+\nu_m)A_5 A]/2A} \tag{2.2.13}$$

$$\frac{G_{12}}{G_m} = 1+\frac{V_f}{\frac{G_m}{G_f+G_m}+2V_m S_{1212}} \tag{2.2.14}$$

$$\frac{G_{23}}{G_m} = \frac{G_{13}}{G_m} = 1+\frac{V_f}{\frac{G_m}{G_f+G_m}+2V_m S_{2323}} \tag{2.2.15}$$

$$\frac{K_{23}}{\bar{K}_m} = \frac{(1+\nu_m)(1-2\nu_m)}{1-\nu_m(1-2\nu_{12})+V_f\{2(\nu_{12}-\nu_m)A_3+[1-\nu_m(1+2\nu_{12})A_4]\}/A} \tag{2.2.16}$$

$$\nu_{12} = \sqrt{\frac{E_1}{E_2}-\frac{E_1}{4}\left(\frac{1}{G_{23}}+\frac{1}{K_{23}}\right)} \tag{2.2.17}$$

$$\nu_{23} = \nu_{13} = \frac{\frac{K_m/G_m}{K_m/G_m+2}(3-4\nu_{12}^2)-1}{\frac{K_m/G_m}{K_m/G_m+2}+1} \tag{2.2.18}$$

In the sequence 2.2.12-2.2.18, A_{1-5} and A are functions of the Eshelby tensor[1]and the Lamé constants of the matrix and inclusions. Moreover, V_f is the volume fraction of the inclusions, S_{ijkl} are the components of the Eshelby tensor and K_m is known as the plain-strain bulk modulus of the matrix. The stiffness and compliance matrices for unidirectional material can now be set up as in section 2.2.

In order to obtain the stiffness matrix for the oriented (but not unidirectional material) the stiffness matrix needs to be averaged according to local orientation. This is done by averaging the properties according to the fibre orientation distribution density, like in Equation 2.2.11. After averaging the involved properties on the micromechanical level, each point of the continuum model has its own stiffness matrix.

[1]The Eshelby tensor is a fourth order tensor that relates the perturbed strain (of the inclusions) to the equivalent transformation strain of the inclusions. The components of the Eshelby tensor depend on the shape of the inclusions and the elastic properties of the matrix. For more information see for example [3].

2.2.3 Eduljee, McCullough and Gillispie model

In the strength analysis an FE programme has been written which solves for the displacements, stresses and strains of each element. This programme uses the fibre orientation tensor, containing information about principal directions and proportion of fibre in each principal direction, to compute the material properties based on an approach presented by Eduljee et al. [4] and McCullough et al. [13]. In this method a modified Eshelby tensor, $\boldsymbol{E}_m^0$, is used to set up the stiffness matrix. First the stiffness matrices for fibre and matrix are set up separately and then the relation

$$\boldsymbol{C}^{ud} = \boldsymbol{C}_m + V_f((\boldsymbol{C}_f - \boldsymbol{C}_m)^{-1} - V_m \boldsymbol{E}_m^0)^{-1} \tag{2.2.19}$$

is used to obtain the stiffness matrix of the unidirectional material.

The final stiffness matrix is obtained from the stiffness matrix for the unidirectional material and the fibre orientation parameters f_p and g_p, as seen in Table 2.2.1. The fibre orientation parameters f_p and g_p depend on the fibre orientation tensor A_{ij} which can be written as

$$A_{ij} = \begin{bmatrix} A_{11} & A_{12} & A_{13} \\ A_{21} & A_{22} & A_{23} \\ A_{31} & A_{32} & A_{33} \end{bmatrix} \tag{2.2.20}$$

In the case of a plane state of stress A_{ij} reduces to

$$A_{ij} = \begin{bmatrix} A_{11} & A_{12} \\ A_{21} & A_{22} \end{bmatrix} \tag{2.2.21}$$

If the fiber orientation tensor is expressed in the material coordinate system such that its normalized basis vectors coincide with the principal directions, A_{ij} becomes

$$A_{ij} = \begin{bmatrix} a_{11} & 0 \\ 0 & a_{22} \end{bmatrix} \tag{2.2.22}$$

and the fiber orientation parameters f_p and g_p can be computed as

$$f_p = 2a_{11} - 1 \tag{2.2.23}$$

$$g_p = \frac{2f_p(7 - 2f_p)}{5(4 - 2f_p)} \tag{2.2.24}$$

Whereby a_{11} thus represents the proportion of fibres that lie in the first principal direction. The elements of the stiffness matrix can then be computed according to table 2.2.1.

Table 2.2.1 Elements of the stiffness matrix by McCullough et al. [13]

$C_{11} = C_{11}^{random} - [dC_{11} + 5dC_{66}]f_p + 5dC_{66}g_p$
$C_{12} = C_{12}^{random} + 4dC_{12}f_p - 5dC_{12}g_p$
$C_{13} = C_{13}^{random} - dC_{13}f_p$
$C_{22} = C_{22}^{random} - [dC_{22} + 5dC_{66}]f_p + 5dC_{66}g_p$
$C_{23} = C_{23}^{random} - dC_{23}f_p$
$C_{33} = C_{33}^{random}$
$C_{44} = C_{44}^{random} - dC_{44}f_p$
$C_{55} = C_{55}^{random} - dC_{55}f_p$
$C_{66} = C_{66}^{random} + 4dC_{66}f_p - 5dC_{66}g_p$

Where

$dC_{ij} = C_{ij}^{random} - C_{ij}^{ud}$

$C_{11}^{random} = C_{22}^{random} = k + u$
$C_{13}^{random} = C_{23}^{random} = l$
$C_{44}^{random} = C_{55}^{random} = g$
$C_{12}^{random} = k - u$
$C_{33}^{random} = n$
$C_{66}^{random} = u$

$k = (1/4)[C_{11}^{ud} + C_{22}^{ud} + 2C_{12}^{ud}]$
$u = (1/8)[C_{11}^{ud} + C_{22}^{ud} - 2C_{12}^{ud} + 4C_{66}^{ud}]$
$l = (1/2)[C_{13}^{ud} + C_{23}^{ud}]$
$g = (1/2)[C_{44}^{ud} + C_{55}^{ud}]$
$n = C_{33}^{ud}$

2.3 Injection moulding simulation

For injection moulding simulation, Autodesk Moldflow is used, see subsection 3.1.1. Moldflow uses the finite element method (FEM) to solve the flow problem described by Navier Stokes equations for simulations in 3D, or the Hele-Shaw equations for simulation in 2D [6, 14]. For 3D simulations it then uses the computed velocity gradient and volume of fluids method [14] to advance the flow front.

The Hele-Shaw equations can be said to describe laminar Stokes flow between two closely spaced parallell plates. From this follows some simplifications such as that flow in the z-direction is neglected, as well as inertia and gravity effects. However, for thin parts of even thickness it is a good approximation. In this work 3D has been chosen in most of the simulations, based on the geometry of the parts studied. For the strength analysis, 2D analysis was used because it simplifies the manual work within Matlab.

2.4 Fibre orientation

A fibre suspensed in a moving fluid tends to align itself along the flow in the case of a shearing flow. Shearing flows can be found close to the walls of the mould, where the velocity gradient is large due to the difference of velocity between the wall and the more or less free flowing midsection. If the flow instead is a stretching flow, the fibres tend to align themselves transversly relative to the flow. See [6] for more information on the general behaviour of flow and fibre orientation. Figure 2.4.1 shows the general orientation of an injection moulded sheet.

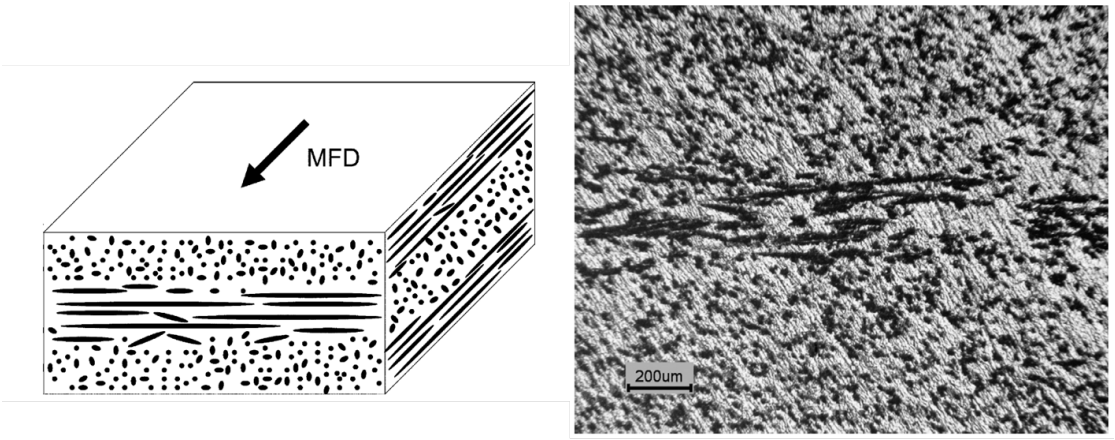

Figure 2.4.1: *Fibre orientation in film gated injection moulded sheet.*[2] *a) Principal orientation of the fibres in the different layers of the sheet and b) Optical microscope observation of polished specimen perpendicular to the flow direction.*

To mathematically describe the orientation of one fibre the vector $\boldsymbol{p}$ is used. For a group of fibres the orientation state can be described by a probability density function $\psi(\boldsymbol{p})$ such that the probability of a fibre having orientation within a small range $d\boldsymbol{p}$ of the direction $\boldsymbol{p}$ is equal to $\psi(\boldsymbol{p})d\boldsymbol{p}$. By integrating over the entire range of p_i the second order orientation tensor, cf. Equation 2.2.20, is given by [1]

$$A_{ij} = \int p_i p_j \psi(\boldsymbol{p}) d\boldsymbol{p} \tag{2.4.1}$$

The tensor A_{ij} thus describes the orientation state of the fibres in one point of the domain. One important characteristic of A_{ij} is that the eigenvectors of A_{ij} represent the principal directions of the material at that point. The normalized eigenvalues represent what proportion of the fibres lie within each principal direction.

The orientation state of fibres in a dilute flow can be obtained from the expression [15]

$$\frac{dA_{ij}}{dt} = (W_{ik}A_{kj} - A_{ik}W_{kj}) + \xi(D_{ik}A_{kj} + A_{ik}D_{kj} - 2A_{ijkl}D_{kl}) \tag{2.4.2}$$

Here W_{ij} is the vorticity tensor, D_{ij} is the rate of deformation tensor and ξ is a shape parameter which is close to unity. This equation is known as the Jeffery form, defining the evolution of the orientation state. However, this particular expression does not correlate very well when there are many fibres in the flow. Folgar and Tucker [16] suggested the addition of a coefficient of interaction, Ci, to account for fibre-fibre interaction.

[2]Reprinted from International Journal of Fatigue, 29, A. Bernasconi, P. Davoli, A. Basile, A. Filippi, Effect of fibre orientation on the fatigue behaviour of a short glass fibre reinforced polyamide-6, pages 199–208, Copyright 2007, with permission from Elsevier.

$$\frac{dA_{ij}}{dt} = (W_{ik}A_{kj} - A_{ik}W_{kj}) + \xi(D_{ik}A_{kj} + A_{ik}D_{kj} - 2A_{ijkl}D_{kl}) + 2Ci\dot{\gamma}(\delta_{ij} - 3A_{ij}) \tag{2.4.3}$$

Ci has a theoretical range of $Ci \in (0, 1)$. Setting $Ci = 0$ reduces the equation to the Jeffrey form. $\dot{\gamma}$ is the shear rate which is computed as the scalar magnitude of D_{ij}. δ_{ij} is the Kronecker delta, defined by

$$\delta_{ij} = \begin{cases} 1 & \text{if } i = j \\ 0 & \text{if } i \neq j \end{cases}$$

For longer fibres such as the ones in the materials studied in this thesis, the Folgar-Tucker model overpredicts the orientation level, according to Autodesk [15], especially near the walls of the mould. Orientation near the walls is highly dependent on the strain of the shearing flow. The Reduced Strain Closure model (RSC) [17] is used by Autodesk. The RSC model is expressed as

$$\frac{dA_{ij}}{dt} = (W_{ik}A_{kj} - A_{ik}W_{kj}) + \xi(D_{ik}A_{kj} + A_{ik}D_{kj} - 2[A_{ijkl} + (1-\kappa)(L_{ijkl} - M_{ijmn}A_{mnkl})]D_{kl}) + 2\kappa Ci\dot{\gamma}(\delta_{ij} - 3A_{ij}) \tag{2.4.4}$$

Setting the Reduced Strain Coefficient $\kappa = 1$ reduces the RSC form to the Folgar-Tucker form above. L_{ijkl}, M_{ijkl} are functions of the orientation state tensor A_{ij}.

Since the Ci-factor has to be measured for a specific material and such data is not available, the last term, the isotropic diffusion term, has been replaced by the Anisotropic Rotary Diffusion model (ARD) [18], giving the equation its final form.

$$\frac{dA_{ij}}{dt} = (W_{ik}A_{kj} - A_{ik}W_{kj}) + \xi(D_{ik}A_{kj} + A_{ik}D_{kj} - 2[A_{ijkl} + (1-\kappa)(L_{ijkl} - M_{ijmn}A_{mnkl})]D_{kl}) + \dot{\gamma}(2[C_{ij} - (1-\kappa)M_{ijkl}C_{kl}] - 2\kappa C_{ii}A_{ij} - 5(C_{ik}A_{kj} + A_{ik}C_{kj}) + 10[A_{ijkl} + (1-\kappa)(L_{ijkl} - M_{ijmn}A_{mnkl})]D_{kl}) \tag{2.4.5}$$

The combination of the ARD and RSC model is called ARD-RSC. The tensor C_{ij}, not to be confused with the stiffness matrix, is a function of A_{ij} and D_{ij}. The expression above contains the fourth order orientation tensor A_{ijkl} which is unknown. It has to be approximated from the second order orientation tensor A_{ij}. This process is called closure approximation and the interested reader is referred to [19] and [20] for more information. In the analyses presented in this thesis the Orthotropic Fitted Closure model (ORF), in Moldflow called Orthotropic 2, has been used.

2.5 Strength

The most common approach when assessing strength of an isotropic material is to use a maximum allowed stress approach. The maximum stress in the material is then compared to the stress limit of the material. The same can be done for strain. In the case of multiaxial load for isotropic cohesive materials the von Mises or Tresca stress can be used. For anisotropic materials this approach is not applicable as anisotropic materials have different strength in different directions, meaning that they fail at different stress levels depending on the direction of the stress. Moreover, the strength of a composite is usually different in compression and tension. For traditional laminate composites this is not too difficult to work around, using a FE analysis program with a composite stacker module and classical laminate theory. It then suffices to know the strength in the different directions of the laminae; the stacker then evaluates when failure will occur in a lamina using a failure criteria. For short fibre composites this issue is more complicated as the failure properties, like the mechanical properties, change over the entire volume of the component.

Laspalas et al. [1] have suggested that an approach similar to the one used to obtain the compliance matrix of the material can be used to establish a strength matrix. The strength matrix for a unidirectional material has the form:

$$F_{ij}^{ud} = \begin{bmatrix} 1/\bar{\sigma}_{cl}^2 & -1/2\bar{\sigma}_{cl}^2 & -1/2\bar{\sigma}_{cl}^2 & 0 & 0 & 0 \\ -1/2\bar{\sigma}_{cl}^2 & 1/\sigma_{ct}^2 & 1/2\bar{\sigma}_{cl}^2 - 1/\sigma_{ct}^2 & 0 & 0 & 0 \\ -1/2\bar{\sigma}_{cl}^2 & 1/2\bar{\sigma}_{cl}^2 - 1/\sigma_{ct}^2 & 1/\sigma_{ct}^2 & 0 & 0 & 0 \\ 0 & 0 & 0 & 2/\sigma_{ct}^2 - 1/\bar{\sigma}_{cl}^2 & 0 & 0 \\ 0 & 0 & 0 & 0 & 2/\sigma_{ct}^2 - 1/\bar{\sigma}_{cl}^2 & 0 \\ 0 & 0 & 0 & 0 & 0 & 1/\tau^2 \end{bmatrix} \tag{2.5.1}$$

Here σ_{cl} is the strenght in the longitudinal direction and σ_{ct} is the strenght in the transverse direction. Since the longitudinal strenght is dependent on the fibre length it is averaged over the fibre length distribution, giving $\bar{\sigma}_{cl}$. As the fibre length distribution is unknown it is assumed constant, which gives $\bar{\sigma}_{cl} = \sigma_{cl}$. τ is the fibre-matrix interface shear strenght.

According to Agarwal et al. [21] the rule of mixtures can be used for a rough estimate of σ_{cl} such that

$$\sigma_{cl} = V_f \sigma_f + V_m \sigma_m \tag{2.5.2}$$

where σ_f and σ_m are the fibre and matrix ultimate strenght respectively. For the transverse strenght the matrix strenght can be used, according to [21], such that

$$\sigma_{ct} = \sigma_m \tag{2.5.3}$$

According to [1], the shear strength, τ, can be estimated by

$$\tau = \frac{\sigma_m}{\sqrt{3}} \tag{2.5.4}$$

For plane stress, rows and columns 3–5 of F_{ij}^{ud} are superfluous and can be removed.

The unidirectional strength matrix gives the strength, of a unidirectional composite, in each direction, just as the unidirectional stiffness matrix gives the mechanical properties of a unidirectional composite, in each direction. However, as in the case of the stiffness matrix, it is the strength matrix of the oriented material, F_{ij}, that is needed. Averaging for fibre orientation is done the same way as in chapter 2.2.3. In this case the strenght matrix is calculated based on the unidirectional strenght matrix F_{ij}^{ud} above, and the fibre orientation data exported from Moldflow. These strength properties can then be compared to the stresses in the model using a failure criterion.

2.5.1 Ultimate strength estimation

To establish the strength matrix the strength of the constituent components is needed. Values for ultimate tensile strength for glass fibres and polypropylene suggest a level of ultimate strain that is way beyond that of the composite. Instead of these values an isotropic Hooke type material model was used, together with data sheet elastic properties of the fibre and matrix, to tune in the failure stress of the test piece. This resulted in failure stresses of each component proportional to 1 % strain, which can be compared to the recorded data sheet failure strain of 1.8 %. This is considered reasonable since the test piece usually will have experienced some plasticity before failure. The ultimate tensile strength values used are found in Table 2.5.1.

Table 2.5.1 Ultimate tensile strenght of composite constituents

	Fail stress [MPa]	Fail strain [%]
E-glass	730	1
Polypropylene	15	1

2.5.2 Failure criterion

There are several failure critera that handle anisotropic strenght and multiaxial loadcases but here the Hill criteria [1] was used because of its mathematical simplicity and easy implementation. The Hill critera is a development of the von Mises critera to account for anisotropy of materials. The Hill failure criteria is expressed such that failure will occur when the left hand side of the equation

$$F_{11}\sigma_1^2 + F_{22}\sigma_2^2 + F_{12}\sigma_1\sigma_2 + F_{21}\sigma_2\sigma_1 + F_{66}\tau_{12}^2 = 1 \tag{2.5.5}$$

exceeds the right hand side.

3 Analyses

The tools, methods and materials used within this thesis work are described in this section. A brief description of the softwares and solvers used is presented and the polymeric material that has been analysed is described. A review of the FE models, including mesh types, boundary conditions and contacts, is made.

3.1 Solver, interface and other software

The main softwares and solvers are presented. Focus of the presentation lies on how the different programmes have been used and what for, but also the experienced strengths and weaknesses in this work.

3.1.1 Moldflow

For the injection moulding simulation Autodesk Moldflow Insight Basic 2012 was used. It is one of the market leading programmes for this purpose and it is widely used in industrial applications.

A Moldflow analysis begins by importing a geometry for the injection moulding and creating an FE mesh for the flow simulation. It is also possible to import, for example, a Patran mesh which can be created in most preprocessors. When using the MSA interface, the model geometry from Abaqus CAE is exported from Abaqus CAE to Moldflow Insight for meshing and analysis. There are three kinds of mesh in Moldflow Insight: Midplane, Dual Domaine and 3D. Midplane is essentially a triangular element shell mesh in which a thickness is assigned, but the model itself has no volume. The solver then uses the Hele Shaw equation for the flow problem which includes a number of, often justified, simplifications, see section 2.3. Dual domaine is a mesh type developed by Moldflow; since this mesh type is unique to Autodesk it has not been used within this work. In 3D the part is meshed with tetrahedral elements and the solver uses the full Navier Stokes equations to predict the flow.

Before running the analysis a material was chosen. Moldflow has an extensive library of polymeric materials and material properties. There is also a number of different options for the fibre orientation solver and micromechanical model. The choices made in this part were motivated in the theory chapter, chapter 2.

It appears that Moldflow can predict fibre orientation and mechanical properties with good accuracy if all related settings are reasonable, and it is easy to use. However, it has its limitations such as the fact that it does not predict ultimate strenght.

Moldflow results, such as the fibre orientation tensor, can be exported as *.xml files which can be read in a text editor or used in for example Matlab. This was done in the strength analysis Matlab programme.

3.1.2 Abaqus

Abaqus 6.10-1 was used as both preprocessor (Abaqus CAE) and solver (Abaqus/Standard) because of the MSA interface with Moldflow. First, the model was preprocessed in the Abaqus CAE environment where the model was meshed, assigned material properties and all loads and boundary conditions were applied. A job was created which was then submitted for analysis using the Abaqus/Standard solver. The Abaqus/Standard solver, as opposed to Abaqus/Explicit, uses implicit integration which makes it stable but less good at solving non-linear and time-dependent problems, none of which was an issue in the current work.

For post processing Abaqus Viewer was used but it could have been any post processor. The post processor enables the user to visually examine the results, such as deformations, stresses, strains, reaction forces etc., and to make any measurements needed.

3.1.3 Moldflow Structural Alliance

There are several different interfaces that transfer mechanical property data from Moldflow to structural analysis solvers such as Abaqus. The one that was used in this work is Autodesk Moldflow Structural Alliance for Abaqus 2012 (MSA for short). It is very easy to use; first the model was prepared in Abaqus CAE and then the geometry was exported to Moldflow. After the injection moulding analysis was run in Moldflow, the Abaqus analysis could be run with the material properties from Moldflow without any additional coding, import or similar.

On the downside there was no possibility to add or change anything in the material data, a feature that could have been used for ultimate strength estimation or nonlinear behaviour. Only linear elastic analyses can be run and only static analyses; this excludes for example transient analysis and eigenfrequency analysis. Also, the part of the structure (in Abaqus called section) that is assigned the Moldflow material properties has to be solid and homogenous, thus one cannot use shell elements [22].

3.1.4 Matlab

As Moldflow currently does not provide ultimate strenght data, a Matlab 7.5 (2007b) routine was written to estimate strengt properties of the injection molded composite. This programme uses the mesh and the fibre orientation data from the Moldflow simulation (using midplane mesh). Material properties were calculated using the programme developed by Oldenbo et al. [23] for fibre orientation averaging based on the equations by McCullough et al. [13]. The programme then uses the Calfem package, v.3.4, [24] to solve the FE problem and visualise the results.

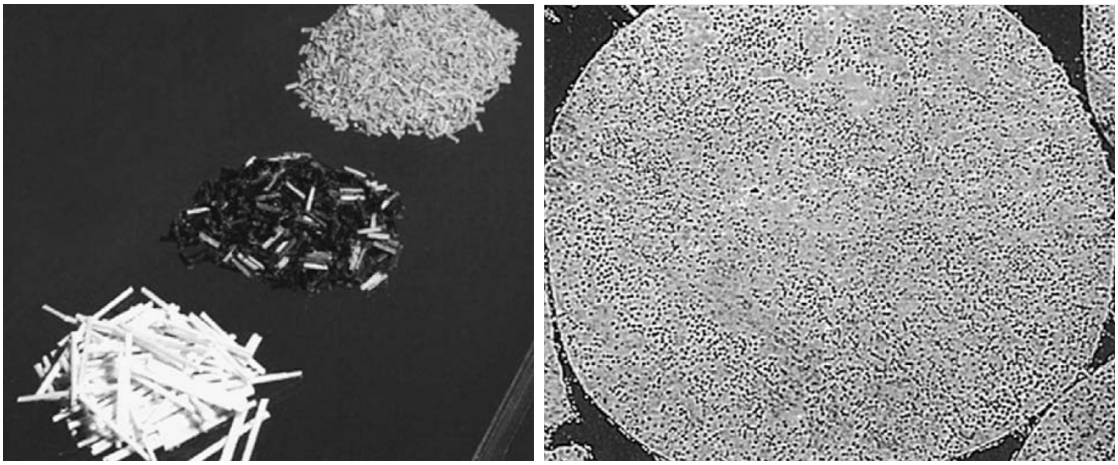

Figure 3.2.1: *Pellets of fibre-reinforced thermoplastics for injection moulding.*[3] *a) Pellets containing fibres of different length and b) Cross-section through a Celstran PP-GF50 pellet showing the separate fibre and matrix phases.*

3.2 Celstran PP-GF50

The polymeric material used in the simulations is Ticona Celstran PP-GF50-03. It consists of a polypropylene matrix reinforced with 50 weight-% glass fibres of 10-12 mm length [8]. The material is provided as pellets which can be injection moulded. The lenght of the pellet is identical to the length of the reinforcing fibres [8]. Figure 3.2.1 shows pellets of different length and a cross-section through a pellet of Celstran PP-GF50. During processing the fibres experience some breakdown due to heat and friction, causing the final composite to have a mean fibre length of about 5-10 mm. The polymer is chemically coupled and heat stabilised. Data sheet values of material properties for Celstran PP-GF50-03 as provided by Ticona [25] are given in Table 3.2.1.

Table 3.2.1 Density and elastic properties of Celstran PP-GF50-03 [25]

Density	1330	kg/m^3
Tensile modulus	10300	MPa
Tensile stress at break	115	MPa
Tensile strain at break	1.8	%
Flexural modulus	10500	MPa
Flexural strength	200	MPa
Charpy notched impact strength	25	kJ/m^2

[3]Reprinted Ticona, Copyright 2000, with permission.

3.3 Structural FE models and preprocessing

For preprocessing of the FE models for structural analysis the preprocessors Ansa and Abaqus CAE were used. In the case of the simple geometries the geometry was created and meshed in Ansa or created in Ansa and meshed in Abaqus CAE. For the case study an existing FE model from [26] was used, and only small changes were made.

3.3.1 Test piece

To verify the methodology a test piece identical to the ISO 527 standard, also used in the Volvo standard VCS 1024 [2], was modelled, see Figure 3.3.1. Test pieces such as this one are injection moulded from one end, giving a rather high level of fibre orientation. The test piece was meshed for structural analysis using 8-noded 3D elements. This test piece was then subjected to a tensile test during which one end was constrained in all degrees of freedom while the other end was displaced 3 mm and the reaction force measured, see Figure 3.3.1. Using the relations:

$$\sigma = \frac{F}{A} \tag{3.3.1}$$

$$\epsilon = \frac{l_1 - l_2}{l_1} \tag{3.3.2}$$

$$E = \frac{\sigma}{\epsilon} \tag{3.3.3}$$

where F is the resulting force in the test piece, A is the cross sectional area of the test piece, l_1 is the test length (approximately the narrow section of the test piece) of the test piece before deformation and l_2 is the length of the same section after deformation, Youngs modulus for the different specimens was calculated.

This analysis was performed on two different material models, both representing the material Ticona Celstran PP-GF50-03, see section 3.2. In the first analysis an isotropic linear elastic material model, using the data sheet value of Youngs modulus as provided by the material supplier, was used. In the second analysis the injection moulding of the test piece was simulated in software package Moldflow, cf. [6], to provide anisotropic, linear elastic material properties for the structural analysis. In the Moldflow simulation a 4-noded 3D tetra element mesh was used. The results of these analyses can be found in subsection 4.1.1. In addition to material properties, Moldflow can also predict process induced stress in the injection moulded part. The impact of process induced stress on the apparent Youngs modulus can be found in Table 4.1.2.

3.3.1.1 Strength analysis

The same test piece as in the stiffness analysis was used to perform a strength analysis in Matlab using fibre orientation data from Moldflow. This time a coarse 3-noded triangle midplane mesh, see subsection 3.1.1, was used for the injection moulding analysis. The

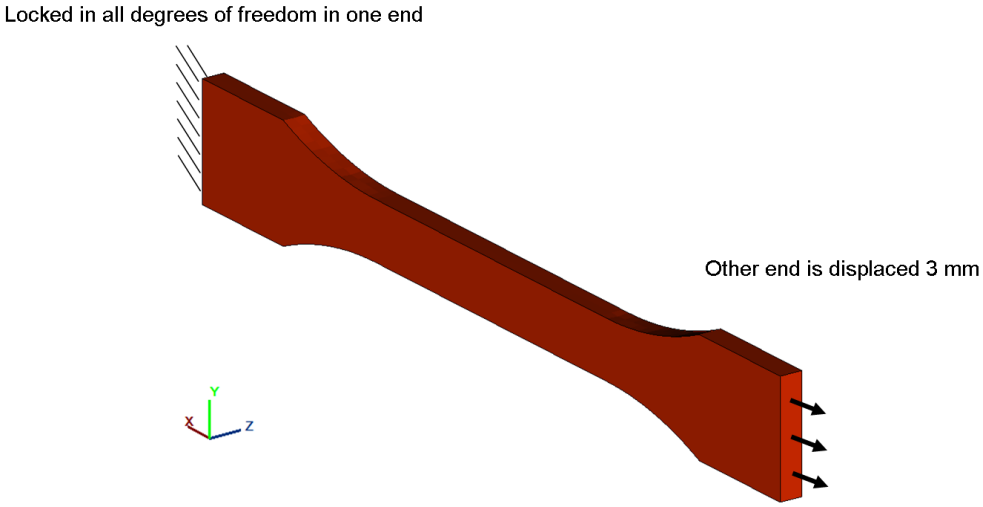

Figure 3.3.1: *Model for simulation of tensile stiffness and strength testing. One end was locked in all degrees of freedom while the other end was displaced. The resulting force was measured and Youngs modulus for the material was calculated.*

same mesh was then exported as a Patran file which, after some rearrangement, could be read into Matlab for the structural analysis. Just like in the previous analysis one end of the test piece was constrained and the other was displaced in the x-direction, see Figure 3.3.1, and the resulting force and deformation registred.

As stated in subsection 2.5.2 the test piece will fail when one of the elements experiences a Hill value exceeding one. The stress and strain of the test piece at which this occurs have been registred and can be found in section 4.2.

3.3.2 Plate with hole

To investigate the effect of anisotropy a geometrically symmetric test geometry was studied. The geometry is a thin square plate with a hole placed in the middle. By placing the injection location for the moulding process on one of the sides of the plate, a rather high level of orientation was obtained. The plate was constrained in all translational degress of freedom along one side and the opposite side was displaced, see Figure 4.1.3. This was performed in both directions and the resulting structural stiffness is shown in subsection 4.1.2.

For the structural analysis the plate was meshed with 8-noded 3D elements; for the Moldflow simulation a 3D tetra mesh was used. Like in the analysis of the test piece two different material models were used, both representing the material Celstran PP-GF50-03, see section 3.2. In the first analysis an isotropic, linear elastic material model with Youngs modulus from the data sheet was used and in the second analysis the material properties from Moldflow were used.

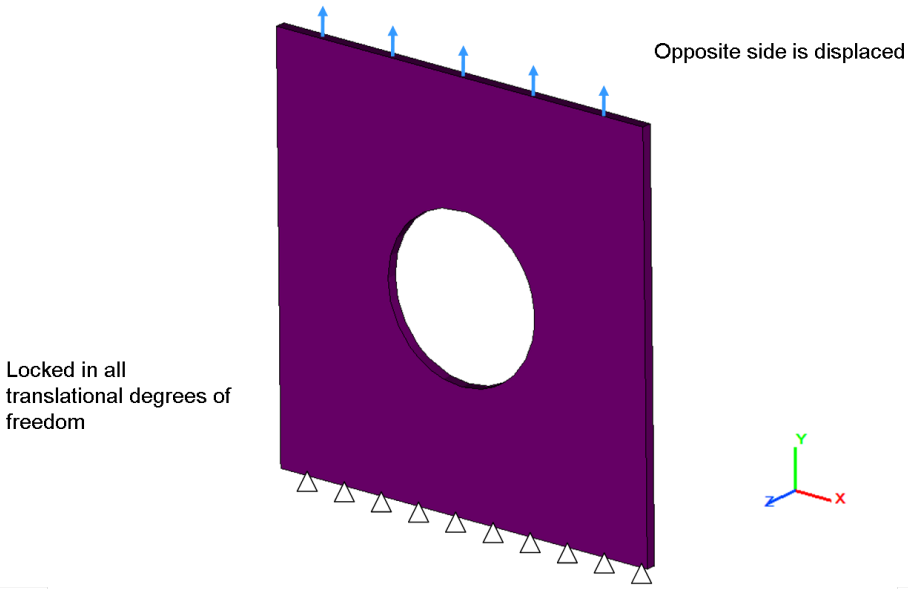

Figure 3.3.2: *Setup of the simulation of the square with hole. One side of the plate was locked in all translational degrees of freedom while the other was displaced. The resulting force was measured. The calculation was performed in both directions to investigate difference in stiffness due to fibre orientation.*

3.3.3 Case study: Battery tray

A structural stiffness analysis of a real component was performed. The geometry is a preproduction status battery tray for the 2012 Volvo V40. The battery tray was injection moulded with Celstran PP-GF50-03, see section 3.2. The geometry was studied in a hypothetical load case in which the battery tray, mounted with a battery weighing approximately 20 kg, was subjected to a gravitational type load and the resulting maximum deflection measured. The tray was locked in all degrees of freedom in three locations, corresponding to where it would be held in place in the actual car. To avoid penetration of the battery into the tray, and for the contact between the tray edge and the battery sides, tie contacts were used. The screw between the steel clamp and the tray was modelled using rigid beam elements. The tray was meshed with solid tetra elements. For the full FE model with all boundary conditions see Figure 3.3.3 and Figure 3.3.4.

Again, the model was analysed using two different material models, the first one being the traditionally employed approach of an isotropic, linear elastic material with Youngs modulus from the data sheet. The second model was the anisotropic material data obtained from the Moldflow simulation. In the Moldflow simulation a 4-noded 3D tetra mesh was used.

The largest deflection of the battery tray was registred and the results can be found in section 4.3.

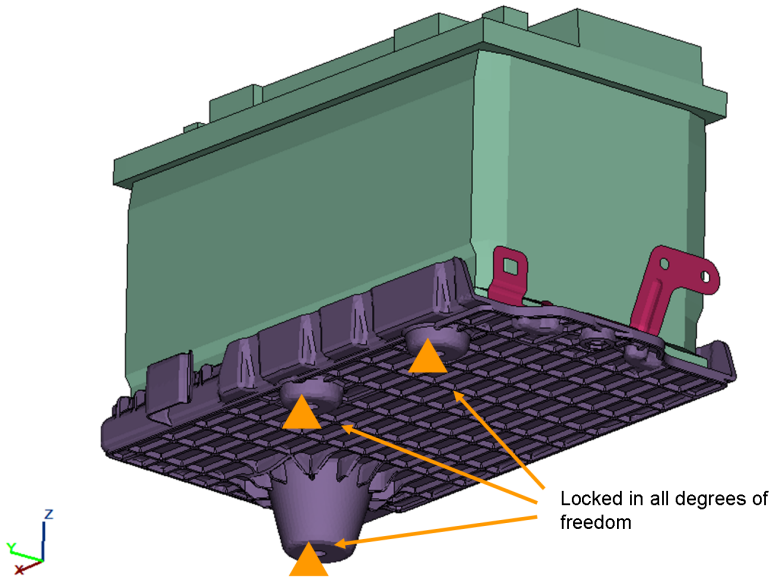

Figure 3.3.3: *Boundary conditions in the case study of battery tray mounted with battery. The tray was locked in all degrees of freedom in locations corresponding to where it would have been mounted in the car.*

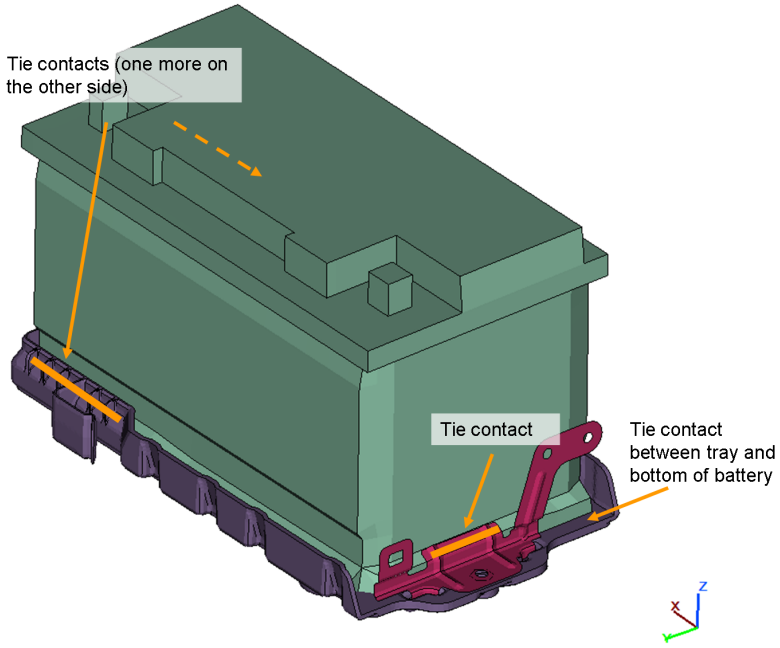

Figure 3.3.4: *Contacts between the tray and the rest of the model. The steel clamp was fastened in the tray using rigid beam elements and tie contacts were used for the contacts between the sides of the tray and the battery, as well as for the contact between the clamp and the battery and between the bottom of the battery and the tray.*

4 Results

The results from the analyses described in chapter 3 are presented. First the results of a simulated tensile test are presented. The correlation between the Youngs modulus found in the data sheet [25] and the Youngs modulus obtained in a simulated tensile test is good, 98 % correlation. Both these moduli were later used as isotropic Youngs modulus for comparison with results obtained when using the anisotropic material properties obtained from Moldflow. Such comparison is made for a simple test geometry as well as for an actual component in a car. Lastly, the results of the strength analysis are presented.

4.1 Linear elastic analysis

Linear elastic analysis was performed for two different test geometries, firstly a test piece according to ISO 527, as also used in the Volvo standard VCS 1024 [2], and secondly a geometrically symmetric square with a centered hole. The results of these analyses were used for comparison with results from tests performed on real test pieces, which are found in data sheets, e.g. [25].

4.1.1 Test piece

ISO 527 test pieces were injection moulded from one end, giving a rather high level of orientation; ∼60–70 % of the fibres lie in the predominant direction, see Figure 4.1.1 and Figure 4.1.2. As can be seen in Table 4.1.1, the correlation between the Youngs modulus found in the data sheets, which are obtained from tensile testing of such test pieces, and the Youngs modulus obtained in simulation of tensile testing is good, 98 % correlation.

To verify the model and setup, the same simulation was performed with the data sheet Youngs modulus, as seen in Table 4.1.1. Table 4.1.1 also shows the Youngs modulus that could be expected based on fibre and matrix moduli if the fibre orientation had been completely random.

Table 4.1.1 Youngs moduli obtained through simulation and testing [MPa] and correlation with respect to data sheet Youngs modulus [ ].

	Using simulated orientation	Simulation using data sheet value	Data sheet value [25]	Assuming random orientation
Youngs modulus	10120	10300	10300†	6300
Corr. wrt †	0.98	1	1	0.61

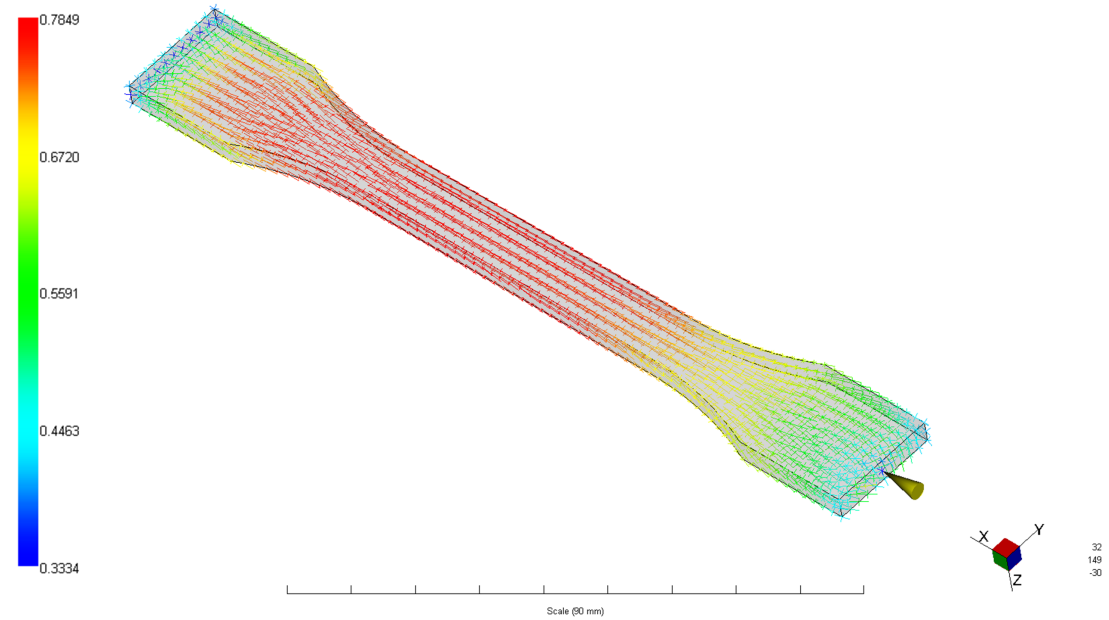

Figure 4.1.1: *Fibre orientation of the injection moulded test piece. The figure shows orientation on the surface. Injection location is marked with the yellow cone.*

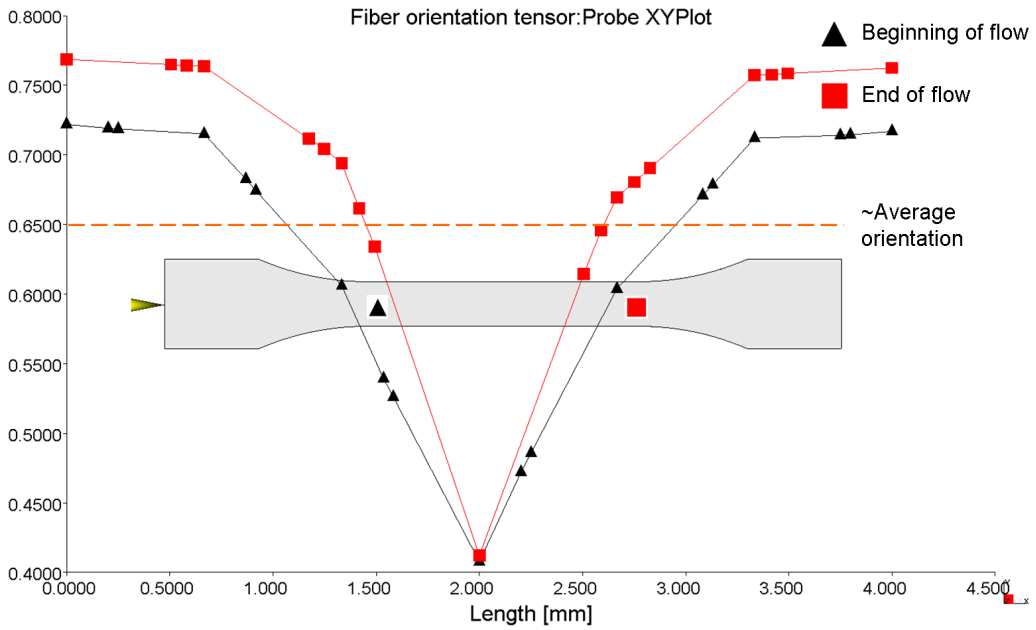

Figure 4.1.2: *Fibre orientation of the injection moulded test piece. The figure shows orientation through the thickness of the part for the two points marked on the test piece in the background. Injection location is marked with the yellow cone.*

4.1.1.1 Process induced stress

Table 4.1.2 shows the resulting Youngs moduli when the test piece has been analysed with and without process induced stress. The first entry represents when process induced stress was not considered at all. The second entry corresponds to a simulation in which the process induced stress was included but the test piece was fully released before subjected to the tensile testing. In the release step the test piece warped somewhat. Length difference between relaxed state and deformed state was measured as well as resultant force in the deformed state. This scenario best describes the actual process.

In the third case the test piece was never relaxed but lenght change was measured from nominal geometry. Resultant force was measured in the deformed geometry. This is considered the least realistic scenario. As can be seen in Table 4.1.2 the difference between case one and two is small.

Table 4.1.2 Apparent Youngs modulus obtained through simulation of tensile test [MPa] and correlation with respect to apparent Youngs modulus obtained without respect to process induced stress [ ].

	w/o initial stress	w relaxation	w/o relaxation
Youngs modulus	10120†	9960	11350
Corr. wrt †	1	0.98	1.12

4.1.2 Square with hole

To see what effect fibre orientation has on global stiffness a geometrically symmetric test geometry was analysed. The results, shown in Table 4.1.3, show that both directions are weaker than what would be expected from the data sheet data. The results using the Youngs modulus found in the data sheet and the Youngs modulus obtained in the tensile test simulation differ the expected 2 %. Note that even the results obtained when using the Youngs modulus for completely random orientation is in the higher range of the results obtained with the material data from Moldflow.

Table 4.1.3 Stiffness of square with hole [N/mm]

	Using simulated orientation	Using Youngs modulus from tensile test simulation	Using Youngs modulus from data sheet	Using Youngs modulus for random orientation
X direction	16600	36400	37200	22600
Y direction	22600	36400	37200	22600

The fibre orientation within the geometry is shown in Figure 4.1.3. The critical region when pulling a geometry such as this is next to the hole. For pull in the y-direction this area appears to have an orientation level of about 0.7, but knowing that orientation is given on the surface of the part the actual orientation level can be expected to be about 0.6 (in first principal direction, which here almost coincides with the y-direction).

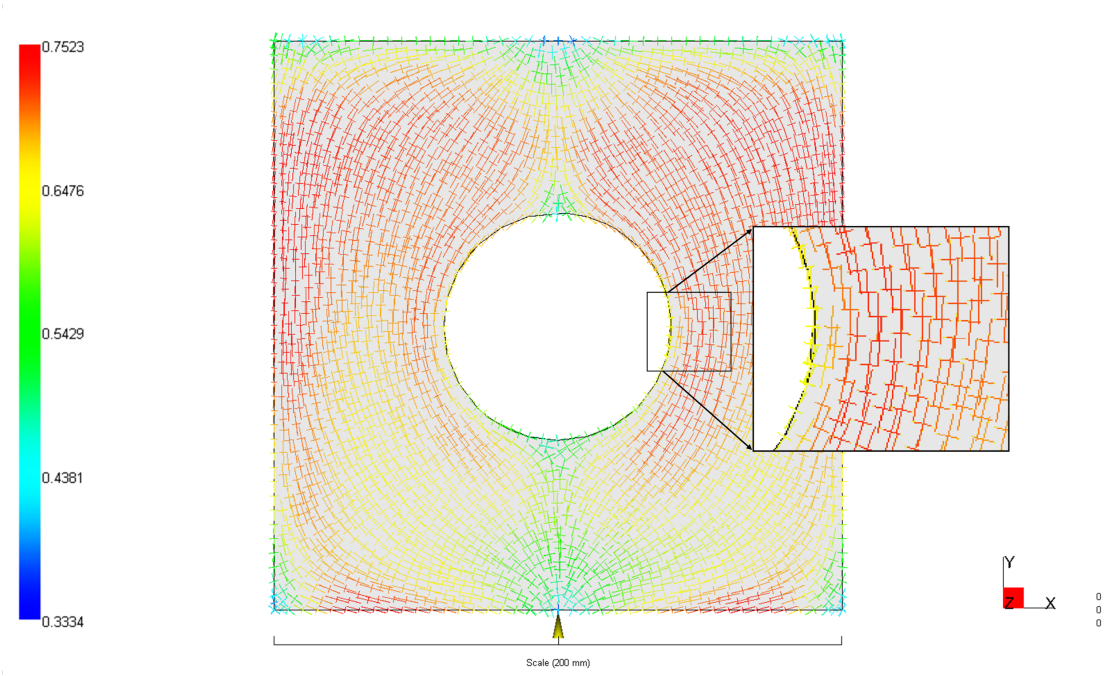

Figure 4.1.3: *Fibre orientation of the injection moulded square with hole. Injection location is marked with the yellow cone.*

For pull in the x-direction the critical area has an orientation level of about 0.6 (in the 1 direction, which here also coincides best with the y-direction). This gives an actual orientation level of about 0.45 in the x-direction. Since the part is thin, only a small proportion of the fibres can be expected to lie in the z-direction so the 1 and 2 directions (the xy-plane) together consist of about 90–100 % of the fibres.

4.2 Strength analysis

A tensile test was simulated until failure was predicted in the first element, based on the Hill criterion. The stress and strain at failure were calculated based on resultant force and elongation as described in subsection 3.3.1. The largest stress and strain experienced by an element were also registred. The fail stress and strain obtained in the strength analysis are shown in Table 4.2.1 together with the stress and strain at break according to data sheet [25]. See subsubsection 3.3.1.1 for more detail on how the routine for strength estimation was constructed.

Table 4.2.1 Stress and strain at the time of failure in the first element

	Using simulated orientation	Data sheet value	Maximum in model
Stress at break [MPa]	118	115	126
Strain at break [%]	1.1	1.8	1.5
Youngs modulus [MPa]	10369	10300	—

The fail stress coincides well with the expected fail stress from the data sheet. For fail strain the correlation is lower which could be explained by, for example, plasticity in the physical test piece. It is worth noticing that the maximum experienced stress in the test piece was higher than the value from the data sheet, and also that there are areas in the part experiencing significantly higher strain than the apparent fail strain, that is, stress and strain along the test piece can be higher than the expected fail stress, yet no failure is predicted by the Hill criteria. Figure 4.2.1 shows a plot of Hill values in the test piece near failure load.

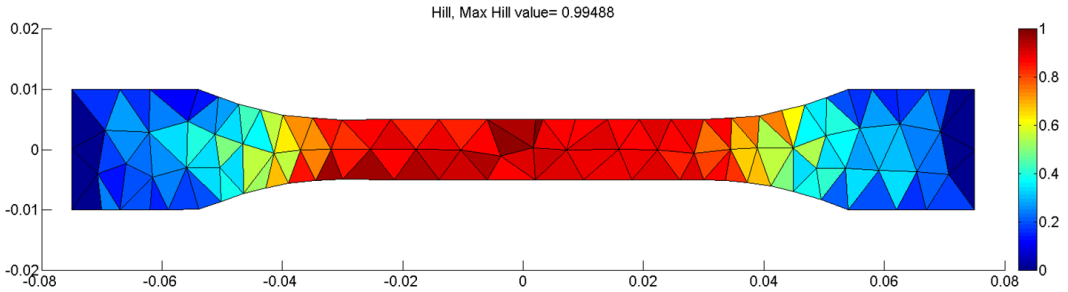

Figure 4.2.1: *Hill plot of the test piece at fail stress. The maximum Hill value in the model is 1.*

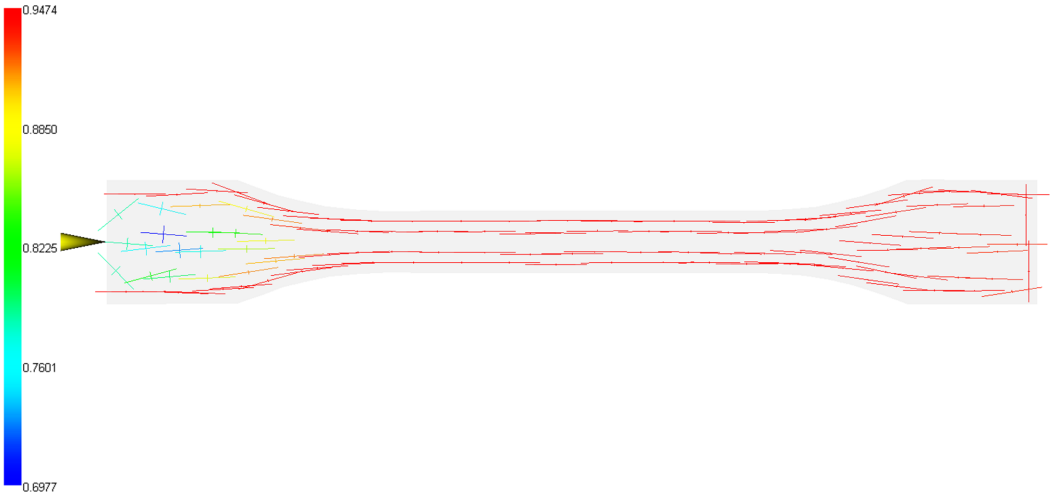

Figure 4.2.2: *Orientation of the test piece when injection moulding is simulated using a Midplane (2D) mesh. Note the scale on the left; the average orientation is significantly higher than in the 3D mesh.*

4.3 Case study: Battery tray

The largest deflection on the bottom of the tray is shown in Table 4.3.1. The tray was analysed with four different material models, while the steel clamp and battery body remained the same.

In the first analysis the material data from Moldflow, which considers process induced fibre orientation, was used. Process induced stress was not included, partly because it was considered to have very little impact on the results, and partly because an existing FE model was used and including process induced stress would mean that the FE model would have to be remade.

These results are compared to the results obtained when using (a) an isotropic material model based on the Youngs modulus from the data sheet, (b) the Youngs modulus that was obtained in the simulated tensile test shown in Table 4.1.1, and (c) the Youngs modulus calculated for a completely random material, seen in Table 4.1.1.

The results show the expected 2 % difference between the data sheet Youngs modulus and the Youngs modulus obtained in simulation of tensile testing in subsection 4.1.1. The Moldflow material on the other hand is significantly weaker than what is predicted using the isotropic assumption. The measured deflection when considering fibre orientation is a factor 1.8 times larger than the deflection predicted when assuming that the material is isotropic, and using Youngs modulus from tensile test or tensile test simulation. A more accurate value is the one obtained when using the Youngs modulus calculated for completely random orientation.

Table 4.3.1 Deflection of battery tray [mm] and correlation with respect to when using Youngs modulus from data sheet [ ].

	Using simulated orientation	Using Youngs modulus from tensile test simulation	Using Youngs modulus from data sheet	Using Youngs modulus for random orientation
Deflection	0.96	0.54	0.53†	0.90
Corr. wrt †	1.8	1.2	1	1.7

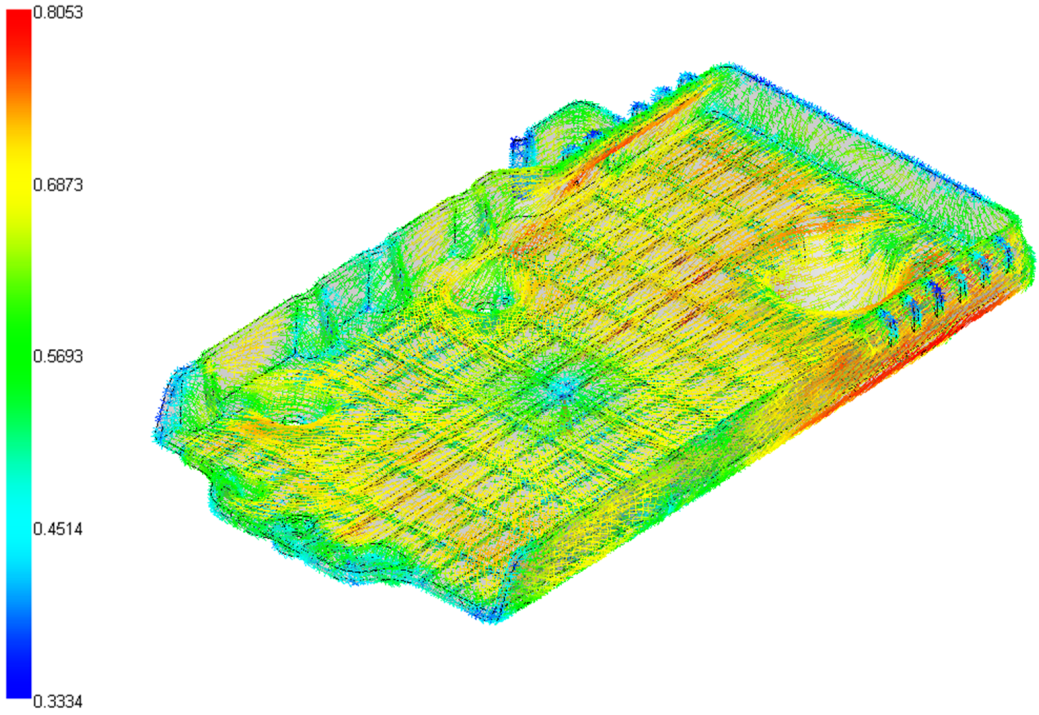

Figure 4.3.1: *Fibre orientation plot of the battery tray. Red areas are highly oriented while blue areas are close to randomly oriented. Note that the first principal direction (which typically is the strongest direction) is directed radially from the injection location, which is located at the bottom of the tray, approximately in the centre.*

5 Discussion

It has been shown that it is possible to use injection moulding process simulation to establish the process induced fibre orientation, and hence predict stiffness and also strength of injection moulded SFC. This has been done both for simple test geometries and real components. In the case study of the battery tray the setup consisted of three different parts, of three different materials. This shows that it is possible to use injection moulding simulations in the regular project work at VCC. Both the results of this work, especially Table 4.3.1, and avaliable research, indicate that it is advisable to consider fibre orientation when analysing SFC, especially ones with longer fibres.

5.1 Stiffness

First of all, the Youngs modulus obtained in the tensile test simulation correlate well with the Youngs modulus of the data sheet. This indicates that the fibre orientation dependent material properties obtained from Moldflow are reliable. The results obtained for less oriented geometries, especially Table 4.3.1, indicate that the stiffness of injection moulded products is overestimated when using stiffness data obtained from oriented test pieces as isotropic material data.

The results are in good agreement with the results obtained by Bernasconi et al. [7], who experimentally found that the stiffness of the 0° orientation is almost a factor 2 larger than the stiffness of the 90° orientation, in a film gated injection moulded sheet. They are also in agreement with the comprehensive data sheets issued by a material supplier, which show that Youngs modulus differ a factor 1.5-1.6 between the directions parallell and orthogonal to the fibre direction [9].

Estimating Youngs modulus for an entirely random material, based on the stiffness and volume fraction of the components, provides a better estimation for Youngs modulus than the data sheet data, and could be sufficient for quick analyses early on in the design process. Later, when accuracy is needed, data from Moldflow or a similar programme can be used for analysis considering process induced fibre orientation. In this work the predicted Youngs modulus for random orientation of 6300 MPa was 39 % lower than the data sheet value of 10300 MPa. In the simulation of the square with hole, even the stiffness predicted when using the calculated Youngs modulus for random orientation was in the higher range of the results obtained when using the material data from Moldflow. One should, however, keep in mind that the difference is small and that the Youngs modulus giving this result is estimated using a different micro mechanical model than the others, indicating that no actual conclusions can be drawn from this.

5.2 Strength

As ultimate strength can be estimated in a similar way as stiffness, orientation dependency can be expected for strength as well. Both Bernasconi et al. [7] and Lutter [9] have

reported a similar or slightly lower difference between longitudinal and transverse direction in strength, than was observed for stiffness. In this thesis the strength properties of the constituents of the composite have been roughly estimated, but the strength of the composite will have to be investigated further. Measuring ultimate strength of the components separately will give an overestimation of the strength of the composite.

Agarwal et al. [21] suggests that longitudinal ultimate strength of a composite can be estimated using the rule of mixtures for the longitudinal strenght, and the matrix strength for the transverse strength. This is the approach that has been used in this work. Others, such as Zenkert and Battley [11], argue that this approach overpredicts the strenght of the composite. The low values of the strain at break for the composite constituents, only 1 %, indicate that perhaps the composite ultimate strenght is underestimated; inaccuracy in ultimate strenght is in fact likely due to uncertainties in ultimate strenght of the constituents. On the other hand, a strain slightly lower than the data sheet value would be expected since the model used takes into account neither plasticity, nor microscopic behaviour such as microcracks or fibre pullout. This is, however, not really an issue since the task was to investigate a method for predicting strength of injection molded short fibre composites based on injection molding simulations, rather than to accurately perform such an analysis.

The fibre orientation obtained from Moldflow for the midplane analysis shows a very high level of orientation, much higher than the 3D simulations performed for the same test piece. To compensate for this a reduction parameter was used within the Matlab script to reduce the orientation to a value closer to what is seen in the 3D simulations and to what correlates well with the stiffness prediction from the Eduljee et al. micro mechanical model [4].

5.3 Process induced stress

During injection moulding, and especially during cooling, the material will build up process induced stresses within the part. When the stresses are released, after some time in room temperatue, they cause the part to warp. As the difference between the simulation without process induced stress and the simulation with relaxation, Table 4.1.2, is less than 2 %, process induced stress has been neglected. It is possible, thought, that for a less oriented geometry, such as the battery tray, these process induced stresses might have a larger impact on the overall stiffness of the part.

5.4 Interface and solvers

Moldflow Insight has a number of features that are of use for designers of injection moulded parts and processes, such as runner and cooling channel design. These features have not been used in this work, since it is the general process of using injection moulding data to predict mechanical behaviour of short fibre reinforced plastics that is of interest rather than using Moldflow as a tool for designing the injection moulding process. For

the same reason process settings such as injection temperature, fill and pack time etc. has been kept at recommended values.

For the daily work within VCC the process followed in this thesis work might cause some difficulties if implemented on a larger scale. It is not preferred that CAE engineers should re-run injection moulding simulations that have already been run by designers in order to obtain material data. The material data might then be less accurate due to simplifications done by the CAE engineer such as neglecting to insert cooling channels or not using the accurate process data. A better approach would be if the CAE engineers get the material data from the designers when they run the sharp simulations. There might be a way around the problem of CAE engineers running Moldflow analyses if there is a strict naming convention and no part is ever reoriented but that seems unresonable. Other interfaces such as for example Simulias Abaqus interface for Moldflow should be investigated.

6 Suggestions for further work

To further increase the knowledge about how fibre orientation impacts ultimate strength a reliable programme must be used. For this purpose the software Digimat ought to be investigated [27]. Digimat claims to contains a more comprehensive material database than Moldflow and uses the fibre orientation state obtained in Moldflow to compute the final material properties. Digimat can therefore predict for example plasticity and ultimate strength when Moldflow cannot. Simulias Moldflow interface for Abaqus might also be of interest, since it provides a more open interface in which it is possible to modify material parameters or to enter custom code.

The results obtained for the simulation of tensile testing of test piece correlate well with the data sheet results. However, it is necessary to test the transverse direction to see if the correlation is good for that direction also. Testing of injection moulded structures should also be performed to see to what extent the global stiffness is accurately predicted by Moldflow.

A thorough correlation of strength properties of the composite and its constituents need to be performed, as this is one of the more uncertain areas in this work. Correlation of strength with respect to physical tests ought also be analysed.

The MSA interface does not work with dynamic analyses, for example eigenfrequency analysis. As eigenfrequencies are highly dependent on material stiffness, this type of analysis would be of interest. It would also be interesting to see if, and to what extent, the eigenmodes change order and/or shape due to the anisotropy of the material.

7 Conclusions

It has been shown in this thesis that it is possible to use injection moulding process simulations to establish the process induced fibre orientation, and hence the resulting elastic and strength material properties of components. This has been done both for simple test geometries, for both stiffness and strength, and for an actual component with respect to structural stiffness. The results have been verified against tensile testing of physical test pieces.

Using process induced fibre orientation to predict stiffness of test pieces has shown very good correlation. For strength as well, the correlation has been good, but the strength analysis contains more uncertainties within both theory and implementation. Strength data for both the fiber and matrix separately, and for the composite, must be evaluated and other Abaqus-Moldflow interfaces, ones that handle strenght data, evaluated.

Youngs modulus of SFC is highly overpredicted in tensile tests with injection moulded test pieces. This makes all computations on short fibre reinforced plastics uncertain. By knowing the fibre orientation and thus the anisotropic material properties, analysis of SFC will become more accurate.

The estimated Youngs modulus for completely random material is a better guess than Youngs modulus obtained in tensile testing of injection moulded test pieces, and might work for early stage analyses. In this work the the predicted value for random orientation of 6300 MPa corresponds to 39 % lower stiffness for a random orientation, compared to the data sheet value of 10300 MPa.

8 List of Figures

1.1.1 Small injection moulding machine for injection moulding of paper clips . . 1
1.1.2 Injection moulded test piece used for tensile testing 2
1.4.1 Work flow of the analyses 4
2.1.1 Different types of fibre composites 5
2.4.1 Fibre orientation in film gated injection moulded sheet 11
3.2.1 Pellets of fibre-reinforced thermoplastics for injection moulding 17
3.3.1 Model for simulation of tensile stiffness and strength testing 19
3.3.2 Setup of the simulation of the square with hole 20
3.3.3 Boundary conditions in the case study of battery tray 21
3.3.4 Contacts between the tray and the rest of the model 21
4.1.1 Fibre orientation of the injection moulded test piece 23
4.1.2 Fibre orientation through the thickness of the test piece 23
4.1.3 Fibre orientation of the injection moulded square with hole 25
4.2.1 Hill plot of the test piece at fail stress 26
4.2.2 Orientation of the test piece simulated using a Midplane (2D) mesh . . . 26
4.3.1 Fibre orientation plot of the battery tray 28

9 List of Tables

2.2.1 Elements of the stiffness matrix 10
2.5.1 Ultimate tensile strenght of composite constituents 14
3.2.1 Density and elastic properties of Celstran PP-GF50-03 17
4.1.1 Youngs moduli obtained through simulation and testing 22
4.1.2 Impact of process induced stress 24
4.1.3 Stiffness of square with hole 24
4.2.1 Strength analysis results 25
4.3.1 Deflection of battery tray 27

10 References

[1] Laspalas M, Crespo C, Jimeenez MA, Garcia B, Pelegay JL. Application of micromechanical models for elasticity and failure to short fiber reinforced composites. Numerical implementation and experimental validation. Computers and Structures. 2008;86:977–987.

[2] VSC 1024, 21119; 2005. VCC Standard for Tensile Strength.

[3] Tandon GP, Weng GJ. The effect of aspect ratio of inclusions on the elastic properties of unidirectionally aligned composites. Polymer Composites. 1984;5:327–333.

[4] Eduljee RF, McCullough RL, Gillispie JW. The influence of aggragated and dispersed textures on the elastic properties of discontinuous-fiber composites. Composites Science and Technology. 1994;50:381–391.

[5] auto motor & sport; 2012. Nr 5.

[6] Learning Autodesk Moldflow Insight Basic -Theory and Concepts 2012; 2011. Autodesk Inc.

[7] Bernasconi A, Davoli P, Basile A, Filippi A. Effect of fibre orientation on the fatigue behaviour of a short glass fiber reinforced polyamide-6. International Journal of Fatigue. 2007;29:199–208.

[8] Celstran Compel Long-fibre-reinforced thermoplastics (LTF); 2000. Publication issued by Ticona.

[9] Lutter F. DurethanBKV 30 Mechanische und thermischeEigenschaften; 2005. Internal document.

[10] Grauers L. Failure analysis of a short fibre composite bumper beam, Master's thesis. Chalmers University of Technology; 2010.

[11] Zenkert D, Battley M. Foundations of fibre composites. KTH Engineering Sciences; 2012. Paper 96-10 2:nd edition revised 2003.

[12] Gibson RF. Principles of composite material mechanics. McGraw Hill; 1994.

[13] McCullough RL, Jarzebski GJ, McGee SH. Constitutive Relationships for Sheet Molding Materials. Proceedings of a Joint US-Italy Symposium on Composite Materials. 1981;p. 261–286.

[14] Patel N. Validation of 3D Moldflow filling analysis for TPV's, Master's thesis. University of Masachusetts Lowell; 2000.

[15] Fiber Orientation Solver Verification and Validation; 2011. Autodesk Inc.

[16] Folgar F, Tucker CL. Orientation behaviour of fibers in concentrated suspensions. Journal of Reinforced Plastics and Composites. 1984;3:98–106.

[17] Tucker CL, Wang J, O'Gara JF. Method and Article of Manufacture for Determining a Rate of Change of a Plurality of Fibers Disposed in a Fluid; 2007. United States patent No. 7,266,469.

[18] Phelps JH, Tucker CL. An anisotropic rotary diffusion model for fiber orientation in short- and long-fiber thermoplastics. Journal of Non-Newtonian Fluid Mechanics. 2009;156:165–176.

[19] Cintra JS, Tucker CL. Orthotropic closure approximations for flow-induced fiber orientation. Journal of Rheology. 1995;39:1095–1122.

[20] Advani SG, Tucker CL. The Use of Tensors to Describe and Predict Fiber Orientation in Short Fibre Composies. Journal of Rheology. 1987;31:751–784.

[21] Agarwal BD, Broutman LJ, Chandrashekara K. Analysis and performance of fiber composites. John Wiley & Sons Inc; 2006.

[22] Autodesk Moldflow Structural Alliance for Abaqus 2012 -Installation and Getting Started Guide; 2010.

[23] Oldenbo M, Mattsson D, Varna J, Berglund LA. Global stiffness of a SMC panel considering process induced fiber orientation. Journal of Reinforced Plastics and Composites. 2004;23:37–49.

[24] Austrell P, Dahlblom O, Lindemann J, Olsson A, Olsson K, Persson K, et al. Calfem -A finite element toolbox, version 3.4. Structural Mechanics, LTH, Sweden; 2004.

[25] Celstran PP-GF50-03 PP Glass Reinforced, data sheet from Ticona; 2007. http://tools.ticona.com/tools/mcbasei/pdf/printpdf.php, downloaded 2012-06-04.

[26] Johansson M. Internal VCC report; 2010. VCC Report No Dura-CAE-2010-069-01.

[27] Kennedy PK. Practical and scientific aspects of injection molding simulation, Ph.D. thesis. Technische universiteit Eindhoven; 2008.